Citation: Molecular Therapy–Nucleic Acids (2012) 1, e29; doi:10.1038/mtna.2012.21

www.nature.com/mtna

AON-mediated Exon Skipping Restores Ciliation in Fibroblasts Harboring the Common Leber Congenital Amaurosis *CEP290* Mutation

Xavier Gerard[1,2], Isabelle Perrault[3], Sylvain Hanein[3], Eduardo Silva[4], Karine Bigot[5], Sabine Defoort-Delhemmes[6], Marlèene Rio[3], Arnold Munnich[3], Daniel Scherman[2], Josseline Kaplan[3], Antoine Kichler[1,2] and Jean-Michel Rozet[3]

Leber congenital amaurosis (LCA) is a severe hereditary retinal dystrophy responsible for congenital or early-onset blindness. The most common disease-causing mutation (>10%) is located deep in intron 26 of the *CEP290* gene (c.2991+1655A>G). It creates a strong splice donor site that leads to insertion of a cryptic exon encoding a premature stop codon. In the present study, we show that the use of antisense oligonucleotides (AONs) allow an efficient skipping of the mutant cryptic exon and the restoration of ciliation in fibroblasts of affected patients. These data support the feasibility of an AON-mediated exon skipping strategy to correct the aberrant splicing.

Molecular Therapy–Nucleic Acids (2012) **1**, e29; doi:10.1038/mtna.2012.21; published online 26 June 2012

Introduction

Retinal dystrophies are the leading cause of incurable blindness in developed countries (prevalence 1/3,000 worldwide). Over the last decade, retinal dystrophies have demonstrated a tremendous clinical, genetic, molecular, and physiopathological heterogeneity.

Leber congenital amaurosis (LCA, MIM204000) is the earliest and most severe of these disorders. With prevalence of 1/60,000 worldwide it is a common cause of blindness in childhood (10%).[1] It is one of the most representative examples of retinal dystrophies heterogeneity. Outcome ranges from severe stationary cone-rod disease with extremely poor visual acuity (VA ≤ light perception; type I) to progressive, yet severe, rod-cone dystrophy with measurable VA in the first decade of life (20/200 ≤ VA ≤ 60/200; type II).[2] Hitherto, 15 disease genes have been identified which account for ~70% of the cases. They are either specifically or preferentially expressed in the retinal pigment epithelium or photoreceptors, or widely expressed.[1,3] This physiopathological heterogeneity challenges the development of therapies with different retinal cell types to be targeted and variable therapeutic windows.

In Western European countries, the centrosomal protein 290 (*CEP290*, MIM610142) is the most common LCA gene (20%)[4,5] and accounts consistently for the most severe disease phenotype (type I).[5] *CEP290* encodes an integral component of the ciliary gate that bridges the transition zone between the cilia and cytoplasm of a broad range of cells including photoreceptors. The protein plays an important role in maintaining the structural integrity of this gate, and thus has a crucial role in maintaining ciliary structure and function.[6] As a result, in addition to LCA, *CEP290* mutations cause a wide range of distinct phenotypes,[7] including Senior-Loken syndrome (*SLNS6*, MIM610189), Joubert syndrome (*JBTS5*; MIM610188), Bardet-Biedl syndrome (*BBS*, 209900), and the lethal Meckel-Grüber syndrome (*MKS4*, MIM611134).

Despite the identification of over 100 unique *CEP290* mutations, no clear genotype-phenotype correlations could yet be established[7] with the exception of the LCA-specific c.2991+1655A>G mutation.[4,5] This single mutation accounts for 10% of cases[5] and represents therefore an important therapeutic target. It is located deep in intron 26 where it creates a splice donor downstream of a strong acceptor splice site. As a result, a cryptic 128 bp exon encoding a stop codon is inserted in the *CEP290* messenger RNA (mRNA).[4]

Considering the potential of exon-skipping as a means to bypass protein-truncation[8–11] resulting from the c.2991+1655A>G mutation, we assessed the efficacy of antisense oligonucleotides (AONs) as splice switching oligonucleotides to correct the abnormal splicing in cell lines of LCA patients harboring the mutation.

Results

Expression levels of *CEP290* mRNAs

Fibroblasts were derived from skin biopsies of controls (C_1–C_4), heterozygous carriers (S_1–S_3), and homozygous (P_1, P_2, and P_4) or compound heterozygous patients (P_3). Expression levels

[1]Genethon, Evry, France; [2]CNRS UMR 8151-Inserm U1022, Université Paris Descarte-Sorbonne Paris Cité, Chimie-Paristech, Paris, France; [3]INSERM U781 and Department of Genetics, Université Paris Descartes-Sorbonne Paris Cité, Institut Imagine, Paris, France; [4]Center for Hereditary Eye Diseases, Department of Ophthalmology, University Hospital of Coimbra, Coimbra, Portugal; [5]Centre d'Exploration et de Ressources Thérapeutiques en Ophtalmologie, CERTO, Paris, France; [6]Service d'Exploration de la Vision et Neuro-Ophtalmologie de l'Hôpital Salengro du CHRU de Lilles, Lilles, France
Correspondence: Jean-Michel Rozet INSERM U781 and Department of Genetics, Université Paris Descartes-Sorbonne Paris Cité, Institut Imagine, 75015 Paris, France. E-mail: jean-michel.rozet@inserm.fr or Antoine Kichler CNRS UMR 8151-Inserm U1022, Université Paris Descarte-Sorbonne Paris Cité, Chimie-Paristech, Paris, France. E-mail: antoine.kichler@parisdescartes.fr
Keywords: antisense oligonucleotide; CEP290; ciliogenesis repair; LCA; splice switching-mediated therapy
Received 29 February 2012; revised 3 May 2012; accepted 3 May 2012; advance online publication 26 June 2012. doi:10.1038/mtna.2012.21

of the wild-type and mutant *CEP290* mRNAs were measured by quantitative reverse transcription PCR (RT-qPCR) in all cell lines. Compared to controls and healthy carriers, patients' fibroblasts expressed reduced yet measurable levels of wild-type mRNAs (mean relative expression levels of 0.72 ± 0.14, 0.46 ± 0.06, and 0.16 ± 0.02 in control, carrier, and patient cell lines respectively; **Figure 1a**). Mutant mRNAs were detected to low levels in patients and heterozygous carriers suggesting degradation through nonsense-mediated mRNA decay (NMD). To assess this hypothesis, we compared the mean level of expression of the mutant and wild-type alleles in the patient P_1 cell line before and after treatment with NMD-inhibitor emetine.[12] The significant increase of mutant but not wild-type mRNA levels in cells treated with emetine supported the view that the aberrant transcript is prone to NMD ($P < 0.003$; **Figure 1b**).

Design of AON

Important parameters including guanine-cytosine content influence efficiency of AONs to induce exon skipping.[13] Nevertheless, the design of AON remains empiric. We designed five 2′-O-methyl-phosphorothioate (2′-OMePs) AONs targeting either the donor site (HD26 (+10−11), HD26 (+19−10), and HD26 (+7−18)) or exonic splice enhancer (ESE) sequences predicted using the ESEfinder program (ESE (+50+70) and ESEbis (+90+120); **Figure 2**).

AON-induced correction of the splice defect

AON efficacy was assessed by RT-qPCR by measuring the level of expression of the wild-type and mutant alleles in control, patient, and carrier cell lines transfected for 24 hours with 150 nmol/l of AON in the cationic peptide LAH4-L1[14] (wt/wt 10/1). The use of AONs resulted in a significant increase in wild-type mRNA levels suggesting their ability to skip efficiently the aberrant transcript (**Supplementary Figure S1**).

The ESE (+50+70) AON was selected for further experiments for its ability to reproducibly induce targeted exon-skipping at high levels (**Figure 3**, **Supplementary Figure S2** and **Supplementary Materials and Methods**).

To assess whether the skipping efficacy was dose-dependent, we treated patient, carrier, and control cell lines with increasing amounts of ESE (+50+70) AON. In carrier- and patient-derived cell lines, expression levels of the wild-type mRNA increased with the amount of AON. At an AON concentration of 150 nmol/l, the wild-type mRNA expression in patient cell lines reached the levels measured in controls (**Figure 4**). In contrast, the expression of the wild-type *CEP290* mRNA was unchanged in control cells whatever the AON concentration indicating that it did not interfere with normal *CEP290* splicing (**Figure 4**).

Furthermore, we showed that the transfection of a sense version of the ESE (+50+70) AON (ESEsense (+50+70)) in patient, carrier, and control cell lines did not interfere with *CEP290* splicing (**Figure 3**).

Fluorescently labeled antisense and sense oligonucleotides ESE (+50+70) were delivered to cell lines of patient P_1 to make sure that these results were not due to reduced delivery of the sense oligonucleotide. Similar transfection efficiencies (>90%) were observed (**Supplementary Figure S3** and **Supplementary Materials and Methods**).

When, patient P_1 fibroblasts were subjected to ESE (+50+70) AON treatment in the presence of emetine, the expression of the wild-type mRNA increased whereas that of the mutant mRNA decreased, supporting the view that restored stable wild-type mRNA resulted from resplicing of the aberrant mutated NMD-prone mRNA (**Supplementary Figure S4**).

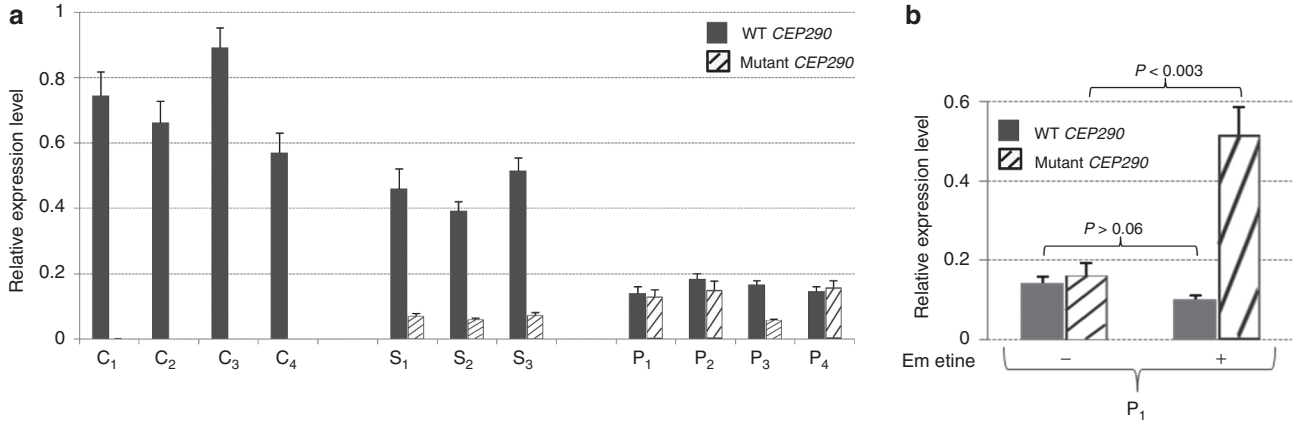

Figure 1 Relative expression of wild-type and mutant (c.2991+1655A>G) transcripts of the *CEP290* gene in patient and control fibroblasts derived from skin biopsies. The error bars represent the SD of the mean derived from three independent experiments. Relative expression levels of wild-type (WT *CEP290*; plain bars) and c.2991+1655A>G mutant (Mutant *CEP290*; hatched bars) mRNAs were determined by RT-qPCR. Results were normalized using the software geNorm. (**a**) Basal expression of *CEP290* mRNAs in untreated cell lines from control individuals (C1–C4), heterozygous unaffected carriers (S1–S3), and LCA patients (P1–P4). A striking reduction in the basal level of expression of the wild-type *CEP290* mRNAs is observed in patient cell lines compared to controls. Results were normalized by using the *RPLP0* and *GUSB* genes as reference. (**b**) Relative expression levels of the wild-type and mutant *CEP290* mRNAs in the fibroblasts of homozygous patient P1, before (–) and after (+) treatment with emetine. The significant increase in expression of the mutant (Mutant *CEP290*; hatched bars), but not the wild-type (WT *CEP290*; plain bars) mRNAs in cells treated with emetine (25 µg/ml) suggests the degradation of the mutant mRNAs through NMD mechanisms. Results were normalized using the *TBP*, *RPLP0*, and *GUSB* genes as reference

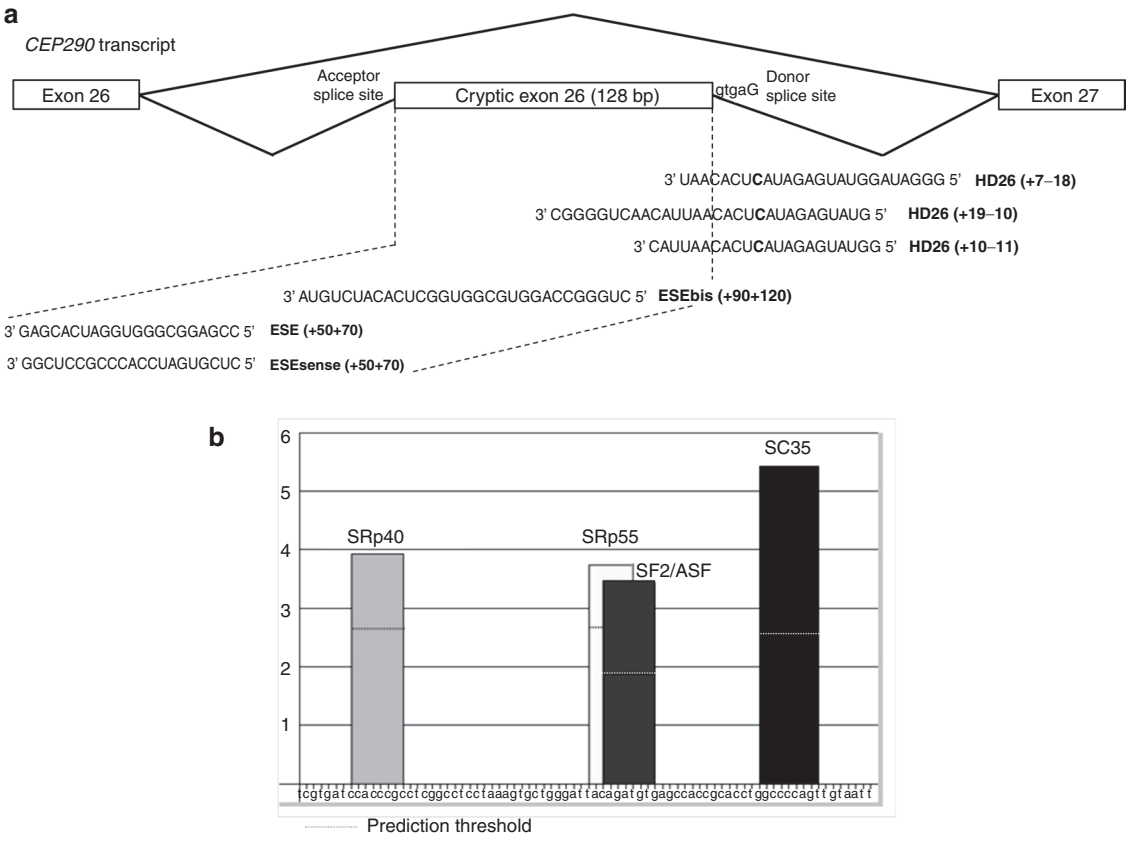

Figure 2 Position of AONs designed to correct the aberrant splicing resulting from the *CEP290* c.2991+1655A>G mutation. (**a**) Schematic representation of wild-type and mutant CEP290 transcripts and sequences of AONs. Five AONs were designed to target the donor splice site and the exonic splice enhancer (ESE) sequences in the cryptic exon using the ESEFinder 3.0 program available at http://rulai.cshl.edu/cgi-bin/tools/ESE3/. The ESEsense oligonucleotide is a sense version of ESE (+50+70). (**b**) Schematic representation of four predicted ESE. The figure shows the results of the analysis of the mutant exon sequence using the ESEfinder web-resource. The x-axis shows a partial sequence of the mutant exon and the y-axis is the numerical scale for the ESE score. Bars represent the four SR proteins (serine/arginine-rich proteins) involved in ESE changes; the mutant exon 26 is expected to contain a SRp40, SC35, SF2/ASF, and a SRp55 protein recognition sites. AON, antisense oligonucleotide.

Finally, RT-qPCR carried out on total RNA extracted from cytoplasmic fractions of treated patient P_1 cell lines detected significant levels of respliced mRNAs supporting transport of corrected mRNA in the cytoplasm (**Supplementary Figure S5** and **Supplementary Materials and Methods**).

Together, these data support dose-dependent and sequence-dependent ability of the ESE (+50+70) AON to induce skipping.

AON-mediated skipping induces increase in *CEP290* concentration and improves ciliogenesis

To assess the effect of AON-induced exon-skipping on the CEP290 protein amount, we performed western blot analyses. A polyclonal anti-CEP290 antibody raised against the carboxy-terminus was used which detects the wild-type but not the mutant CEP290 protein.

Transfection of patient and carrier cells using the ESE (+50+70) AON showed efficient exon-skipping at the mRNA level (**Figure 5**). Western blot analyses of the transfected cells showed that ESE (+50+70) AON delivery resulted in an increased amount of the CEP290 protein (**Figure 5**). These data give strong support to the view that the increase in the wild-type transcript abundance results in an increase of protein concentration.

Considering the role of CEP290 in cilia assembly and/or maintenance,[6] patient and control cell lines were subjected to a 30 hours-serum starvation to assess their respective ability to build a primary cilium. Significantly reduced primary cilia expression was found in patient cell lines compared to controls (mean 48.6 ± 6.5% versus 83.6 ± 3.2% in controls; $P = 0.0097$; **Figure 6**).

Interestingly, transfection of the antisense but not the sense oligonucleotide increased cilia expression to control levels, suggesting improved ciliation (mean 75.3 ± 3.5% versus 78.3 ± 3.4% in controls; $P = 0.624$) (**Figure 6**).

Discussion

Mis-splicing is among the most frequent pathogenic mechanisms underlying genetic diseases.[15,16] Strategies have been developed which allow the modification of splice patterns of genes to overcome pathogenic process leading to disease

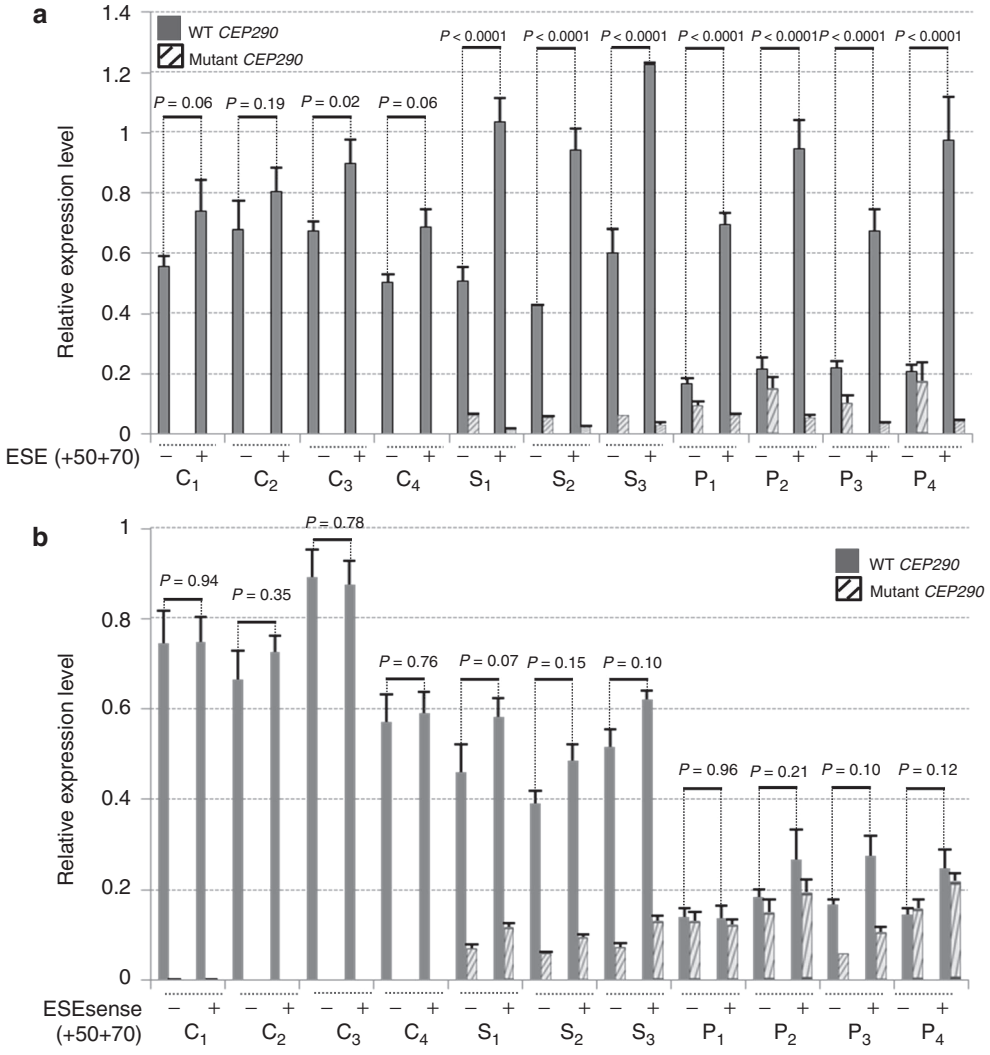

Figure 3 Effect of AON-mediated exon-skipping of the mutant cryptic *CEP290* exon on messenger RNAs (mRNAs). All measures were recorded in untreated (–) or treated (+) fibroblasts derived from skin biopsies of control individuals (C_1–C_4), heterozygous unaffected carriers (S_1–S_3), and/or LCA patients (P_1–P_4). The error bars represent the standard deviation of the mean derived from three independent experiments. Relative expression levels of wild-type (WT *CEP290*; plain bars) and c.2991+1655A>G mutant (Mutant *CEP290*; hatched bars) mRNAs were determined by RT-qPCR. Results were normalized using the software geNorm taking as reference the *RPLP0* and *GUSB* genes. Basal expression levels of wild-type *CEP290* mRNAs were strikingly reduced in patient cell lines compared to controls. Transfections with the (**a**) antisense, but (**b**) not the sense, oligonucleotide ESE (+50+70) resulted in a statistically significant increase in the expression of the *CEP290* wild-type mRNA in patients and heterozygous carriers (P < 0.0001). AON, antisense oligonucleotide; ESE, exonic splice enhancer; LCA, Leber congenital amaurosis; RT-qPCR, quantitative reverse transcription PCR.

drugs, isoform-specific antibodies, trans-splicing approaches, RNA interference and AONs have been investigated for their ability to modify splicing in various diseases.[15–19] Compared to most other molecules, nuclease-protected phosphorothioate AONs are of easy design[13] and inexpensive. In addition, these splice switching AONs can be widely used to restore a wild-type genetic configuration by allowing the skipping of stray pseudoexons that are relatively common in most genetic diseases;[15] 2′-OMePS AONs have been primarily used to treat acute diseases over a period of weeks or occasionally months.[15] Now, clinical trials aiming at assessing lifelong treatments of various genetic diseases are ongoing.[15] Current ongoing trials in patients affected with Duchenne muscular dystrophy have shown that short-term treatment using 2′-OMePS AONs is well tolerated.[9,20,21]

With respect to diseases affecting vision, it is worth remembering that because the eye is easily accessible, small, confined, and has an efficient blood-retina barrier, it is regarded as an ideal target organ for topical treatment. So far, to our knowledge the use of 2′-OMePS AONs is restricted to the treatment of acute cytomegalovirus retinitis using the FDA approved Vitravene.[22] Considering inherited diseases of the retina, the promising clinical trial phase of gene therapy for LCA due to *RPE65* mutations have triggered efforts in developing similar treatments.[23] *CEP290* replacement, whose development would benefit from

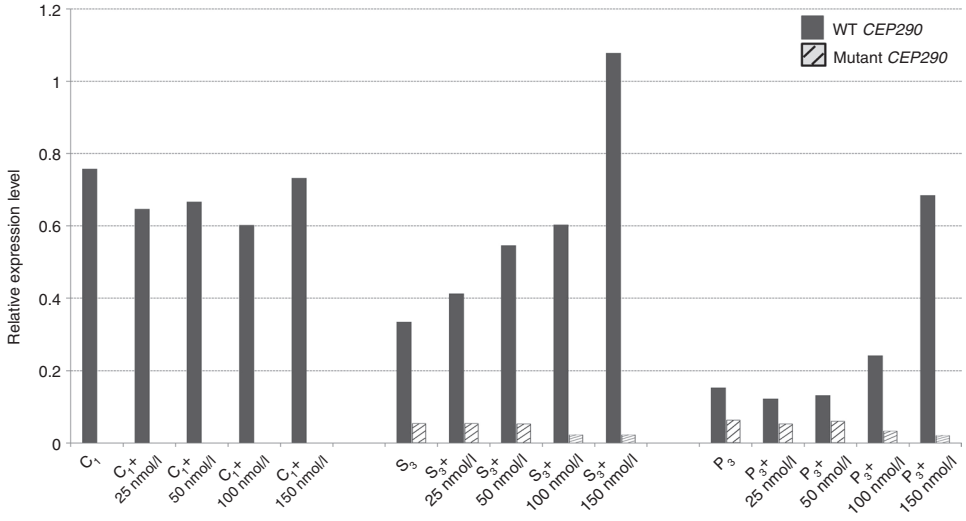

Figure 4 Optimization of transfection conditions. RT-qPCR analysis after transfection of increasing doses of ESE (+50+70) AON with the peptide LAH4-L1 in control (C_1), unaffected carrier (S_3), and patient (P_3) cell lines, respectively. The graph shows the amounts of wild-type (WT *CEP290*; plain bars) and mutant transcripts (Mutant *CEP290*; hatched bars). Results of real-time PCR were normalized using the geNorm software taking as reference two genes, *RPLP0* and *GUSB*. AON, antisense oligonucleotide; ESE, exonic splice enhancer; RT-qPCR, quantitative reverse transcription PCR.

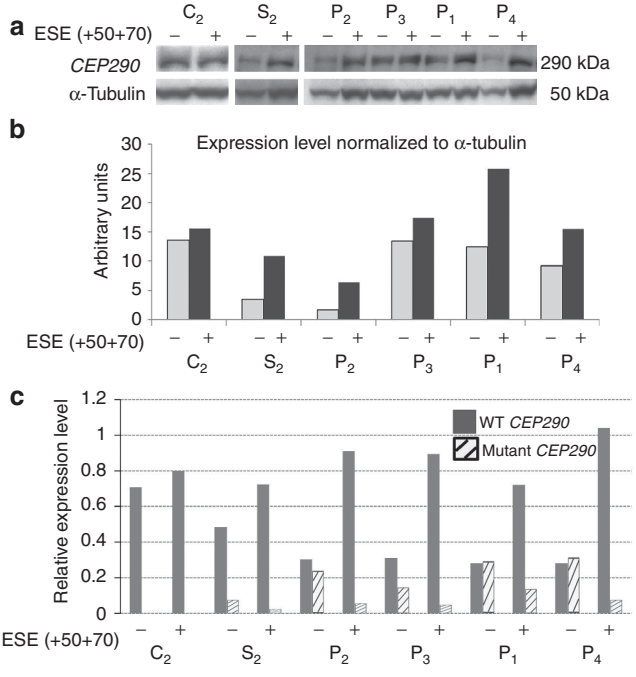

Figure 5 Effect of AON-mediated exon-skipping of the mutant cryptic *CEP290* exon on the protein. (**a**) The expression of the CEP290 proteins in cell lines before (–) and after treatment (+) with the ESE (+50+70) AON was determined by western blot. (**b**) The relative variations in CEP290 expression were determined by computed-densitometry analysis of CEP290 and α-tubulin expression in each sample. (**c**) Relative expression levels of wild-type (WT *CEP290*; plain bars) and c.2991+1655A>G mutant (Mutant *CEP290*; hatched bars) mRNAs were determined by RT-qPCR. Results were normalized using the geNorm software taking as reference the *TBP*, *RPLP0*, and *GUSB* genes. RT-qPCR analysis of patient samples used for western blot analysis confirmed efficient exon-skipping in all treated cell lines. AON, antisense oligonucleotide; ESE, exonic splice enhancer; mRNA, messenger RNA; RT-qPCR, quantitative reverse transcription PCR.

available spontaneous animal models mimicking the human disease (*rd16* mouse and *rdAc Abbyssinian* cat),[24,25] is an attractive option to treat LCA patients harboring *CEP290* mutations, including the common c.2991+1655A>G mutation. However, *CEP290* may be expressed in at least 11 alternative transcripts most of which are predicted to encode proteins whose tissular expression and function are unknown (http://harvester4.fzk.de/harvester/human/IPI00794/IPI00794668.html). Restoring the wild-type genetic configuration by correcting the aberrant splicing resulting for the c.2991+1655A>G mutation may thus be regarded as a preferable option.

Here, we show that this strategy is efficient to correct abnormal splicing accounted for by the *CEP290* c.2991+1655A>G mutation in fibroblasts cell lines obtained from LCA patients. Interestingly, AONs complementary to either the splice donor or exonic splice enhancer sites cause a three to 4.5-fold upregulation of wild-type mRNA in patient-derived fibroblasts to levels equaling that in wild-type cells indicating a significant degree of flexibility in the design of future therapeutic oligonucleotides.

Western blot analyses indicated that despite significant upregulation of wild-type mRNA in patient cells, as measured by RT-qPCR, protein levels were moderately increased (**Figure 5**). Discrepancies between have been previously reported.[26,27] Slow synthesis of large proteins, post-transcriptional, and post-translational regulations have been considered to explain these discrepancies.[28,29] Considering that the increase in restored stable wild-type CEP290 mRNA arises from nuclear resplicing of the aberrant mutated NMD-prone mRNA (**Supplementary Figure S4**) and that significant levels of respliced mRNA were measured in cytoplasmic fractions of AON-treated cells (**Supplementary Figure S5**), these hypotheses are likely to account at least in part to the discrepancy between mRNA and protein abundance increase.

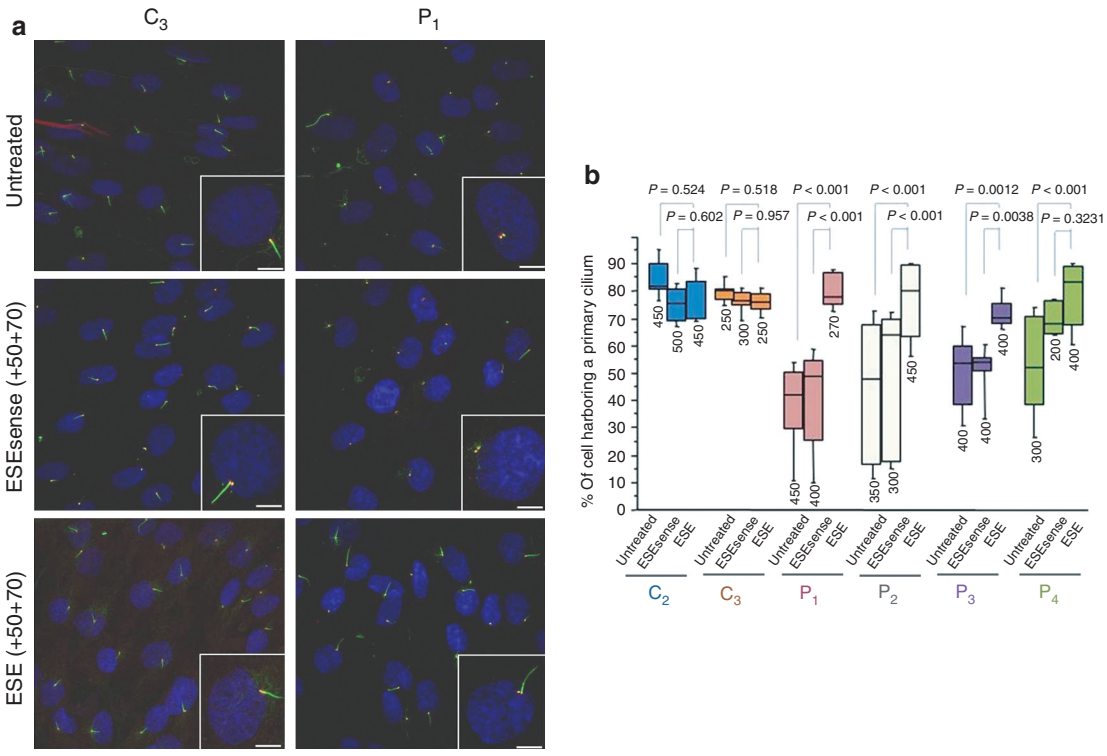

Figure 6 Effect of exon-skipping on ciliogenesis. (a) Nuclei, cilia, and basal bodies of untreated cell lines and fibroblasts transfected with the ESEsense(+50+70) or ESE(+50+70) oligonucleotides were labeled using DAPI (blue), anti-acetylated–tubulin (green). and anti-γ–tubulin (red) antibodies, respectively (right panel). Bar = 5 µm. (**b**) The proportions of fibroblasts presenting a primary cilium among cells were calculated by numbering at least 200 cells in at least four fields (mean $n = 9$) from two independent experiments. AON-mediated exon-skipping of the mutant cryptic *CEP290* exon on messenger RNAs resulted in increased proportions of cells harboring a primary cilium for all four patients (statistically significant in 3/4 patients' cell lines P_1, P_2, P_3). Data are presented using bowplot graphical view. Line running horizontally within the box represents the median. The upper and lower limits of the box are formed by 25th (lower quartile Q1) and 75th (upper quartile Q3) percentile values, respectively. The tips of the whiskers extending from the box are the smallest and the largest observations, respectively. Statistical analyses were carried out by analysis of variance (ANOVA) and PLSD Fisher test (ANOVA, Statview Software, version 5). AON, antisense oligonucleotide; DAPI, 4′,6-diamidino-2-phenylindole; ESE, exonic splice enhancer; PLSD, protected list significant difference.

Recently, we reported that *CEP290* mutations, including the c.2991+1655A>G change, are expressed in nasal epithelial cells of LCA patients.[30] In accordance with the function of CEP290 in cilia assembly and/or maintenance,[6] we evidenced consistent ciliary defects in nasal ciliated cells of patients. Most of these cells presented reduced numbers of cilia, most of which were shorter than normal and presented various axonemal defects.[30] We report here, that in contrast to control cells, high numbers of patient cells display no primary cilium even after a 30 hours-serum starvation, suggesting that the *CEP290* c.2991+1655A>G mutation alters the ciliation process in the cells. Most interestingly, the results we report here show that, despite a moderate increase in protein abundance compared to respliced mRNAs, the use of AON is able to improve significantly ciliation in patient cell lines supporting the therapeutic potential of this strategy.

Finally, the efficiency and absence of major side-effect of intravitreal injections of FDA-approved Vitravene[22] to treat acute cytomegalovirus retinitis is an encouragement to continue the development of this promising AON-induced exon-skipping strategy to bypass the most common LCA-causing mutation.

Materials and methods

Transfection agent and AONs. The 26 residues long cationic transfecting peptide LAH4-L1[14] (KKALLAHALHLLALLAL-HLAHALKKA) was prepared by automated solid-phase synthesis on Millipore 9050 or ABI 431 synthesizers using Fmoc Chemistry (a kind gift by Andrew J. Mason and Burkhard Bechinger). The 2′-O-methyl RNA phosphorothioate oligonucleotides were obtained from Sigma-Aldrich (St Quentin Fallavier, France) (**Figure 2**).

Cell culture and transfection of AONs. Skin biopsies were obtained from four LCA patients harboring the c.2991+1655A>G mutation (3/4 homozygous, P_1, P_2, P_4; 1/4 compound heterozygous with the c.5850delT, p.Phe1950LeuFsX14 mutation P_3), three heterozygous unaffected carriers (S_1–S_3), and control individuals (C_1–C_4). Written informed consent was obtained for each individual and research was approved by institutional review board. Primary fibroblasts were isolated by selective trypsinization and proliferated at 37 °C, 5% CO_2 in Opti-MEM Glutamax I medium (Invitrogen, St Aubin, France) supplemented with 10% fetal bovine serum (Invitrogen), 1% ultroser G

substitute serum (Pall, Saint-Germain-en-Laye, France), and 1% streptomycin/penicillin (Invitrogen). Fibroblasts between passage 7 and 9 were plated at 4 × 10^5 cells/well in 6-well plates 24 hours before transfection. Cells at 80% confluence were transfected with 2′-OMePS AONs (150 nmol/l) in Opti-MEM using LAH4-L1 at a 1:10 (wt:wt) AON:peptide ratio. After 3 hours of incubation at 37 °C, the transfection medium was replaced by fresh culture medium. For the inhibition of NMD, 25 µg/ml of emetine dihydrochloride hydrate (Sigma-Aldrich) was added to the fresh culture medium for 12 hours.

RNA extraction and cDNA synthesis. Twenty-four hours after transfection, the transfected and untreated cells were processed. Total RNA was extracted using the RNeasy Mini Kit (Qiagen, Courtaboeuf, France) according to manufacturer's protocol. All samples were DNase treated by the RNase-free DNase set (Qiagen, Courtaboeuf, France). Concentration and purity of total RNA was assessed using the Nanodrop-8000 spectrophotometer (Thermo Fisher Scientific, Illkirch, France) before storage at –80 °C. Qualitative analysis of total RNA was performed using the Bioanalyzer 2220 (RNA 6000 Nano kit; Agilent Technologies, Massy, France) to verify that the RNA integrity number was between 8 and 10. First-stranded cDNA synthesis was performed from 500 ng of total RNA extracted using Verso cDNA kit (Thermo Fisher Scientific) with random hexamer:anchored oligo(dT) primers at a 3:1 (vol:vol) ratio according to the manufacturer's instructions. A non-RT reaction (without enzyme) for one sample was prepared to serve as control in RT-qPCR experiments.

RT-qPCR. To measure the level of expression of *CEP290* mRNAs, the wild-type and mutant transcripts were amplified as 93 and 117 bp fragments, respectively. Regions of 132, 80, 84, 101, and 95 bp within the human TATA box-binding protein mRNA (*TBP*, NM_003194), the human β-2-microglobulin mRNA (*B2M*, NM_004048.2), the human β-glucuronidase mRNA (*GUSB*, NM_000181.3), the human hypoxanthine phosphoribosyltransferase 1 mRNA (*HPRT1*, NM_000194), and the human P0 large ribosomal protein mRNA (*RPLP0*, NM_001002.3) were used for normalization, respectively. A 99 bp fragment of the human albumin gene (*ALB*, NM_000477) was used to control the non-contamination of cDNAs by genomic DNA. Primers were designed using the Oligo Primer Analysis Software v.7 available at http://www.oligo.net. The specificity of primer pairs to PCR template sequences was checked against the NCBI database using the Primer-BLAST software (http://www.ncbi.nlm.nih.gov/tools/primer-blast). Primer sequences were as follows: *CEP290wt* forward, 5′-tgactgctaagtacagggacatct tg-3′; *CEP290wt* reverse, 5′-aggagatgttttcacactccaggt-3′; *CEP290mt* forward, 5′-ctggccccagttgtaatttgtga-3′; *CEP290mt* reverse, 5′-ctgttcccaggcttgttcaatagt-3′; reference genes *TBP* forward, 5′-tgcacaggagccaagagtgaa-3′; *TBP* reverse, 5′-caca tcacagctccccacca-3′; *B2M* forward, 5′-cctggaggctatccagcgt act-3′; *B2M* reverse 5′-tcaggaaatttgactttccattctct-3′; *GUSB* forward, 5′-gcggtcgtgatgtggtctgt-3′; *GUSB* reverse, 5′-gtgagc gatcaccatcttcaagt-3′; *HPRT1* forward, 5′-accagtcaacaggg gacataaaagta-3′; *HPRT1* reverse, 5′-tttgccagtgtcaattatatct tcca-3′; *RPLP0* forward, 5′-ttctcgttcctggagggtgt-3′; *RPLP0* reverse, 5′-cgttgatgatagaatggggtactgat-3′; *ALB* forward 5′-a tatttccttgtcatcagggttcaga-3′; *ALB* reverse 5′-accttattggatagc ccagatacaga-3′.

cDNAs (5 µl of a 1:25 dilution in nuclease-free water) were subjected to real-time PCR amplification in a buffer (20 µl) containing MESA BLUE qPCR Master Mix Plus for Sybr Assay (Eurogentec, Angers, France) and 300 nmol/l of forward and reverse primers, on a Taqman 7900 HT Fast Real-Time PCR System (Applied Biosystems, Courtaboeuf, France) under the following conditions: Taq polymerase activation and initial denaturation at 95 °C for 5 minutes, followed by 50 cycles for 15 seconds at 95 °C, and 1 minute at 65 °C. The specificity of amplification products was determined from melting curve analysis performed at the end of each run using a cycle at 95 °C for 15 seconds, 65 °C for 15 seconds, and 95 °C for 15 seconds. Data were analyzed using the SDS 2.3 software (Applied Biosystems).

For each cDNA sample, the mean of quantification cycle (Cq) values was calculated from triplicates (SD <0.5 Cq). *CEP290* expression levels were normalized to the "normalization factor" obtained from the geNorm software for Microsoft Excel[31] which uses the most stable reference genes and amplification efficiency estimates calculated for each primer-pair using fourfold serial dilution curves (1:5, 1:25, 1:125, 1:625). No reverse transcriptase (non-RT), no template control (NTC) reactions, and non-contamination of cDNAs by genomic DNA (ALBh) were used as negative controls in each run (Cq values NTC = undetermined, non-RT >40 and ALBh >40).

The quantitative data are the means ± SEM of three independent experiments and these are presented as ratio among values for individual mRNAs. The significance of variations among samples was estimated using the protected list significant difference of Fisher according to the significance of analysis of variance test (Statview Software, version 5; SAS Institute, Cary, NC).

Western blot analysis. Cells were harvested 24 hours after transfection and lysed in a Triton/SDS buffer (25 mmol/l Tris-base pH 7.8, 1 mmol/l DTT, 1 mmol/l EDTA, 15% Glycerol, 8 mmol/l $MgCl_2$, 1% Triton, and 1% SDS) containing complete protease inhibitor cocktail (Roche, Boulogne-Billancourt, France) on ice for 30 minutes with repeated mixing. Released DNA was fragmented by 20 seconds of Ultra-turrax homogenizer (Ika-Werke, Staufen, Germany) and the lysates were centrifuged (15,000*g* at 4 °C for 10 minutes). Protein concentrations were determined from the detergent-soluble fractions using the DC Protein Assay kit according to the manufacturer protocol (Bio-Rad, Marnes la Coquette, France). Proteins (125 µg) were denatured at 90 °C for 10 minutes in 4X premixed protein sample buffer (XT sample Buffer; Bio-Rad) and separated by electrophoresis (50 V for 30 minutes followed by 140 V for 90 minutes at room temperature) on NuPAGE 3–8% Tris Acetate gels (Invitrogen). Proteins were transferred (100 V, 2 hours at 4 °C) to Immobilon-P PVDF membranes (Millipore, Molsheim, France). Membranes were blocked with phosphate-buffered saline (PBS) 0.5% Tween-20/5% dry milk powder and incubated overnight at 4 °C under agitation with polyclonal rabbit anti-human CEP290 (Novus Biologicals,

Littletown, CO) or monoclonal mouse anti-α-tubulin (Sigma-Aldrich) primary antibodies in 1:1,800 and 1:500,000 dilutions, respectively. Membranes were washed three times in PBS 0.5% Tween-20 solution (15 minutes) and incubated for 1 hour at room temperature with HRP-conjugated donkey anti-rabbit and sheep anti-mouse immunoglobulins secondary antibodies (Amersham GE Healthcare, Courtaboeuf, France) in 1:10,000 dilutions, respectively. ECL Western Blotting Detection Reagents (Amersham GE Healthcare) was applied according to the manufacturer's instructions and the blot was exposed to Amersham Hyperfilm ECL (Amersham GE Healthcare). The relative expression of the CEP290 protein was estimated by densitometry using α-tubulin as reference on a G:Box from Syngene with the GeneSnap and GeneTool Softwares.

Immunofluorescence microscopy. Fibroblasts were seeded at 2.5×10^5 cells/well on glass coverslips in 12-well plates, 24 hours before transfection with the ESEsense (+50+70) and ESE (+50+70) oligonucleotides, in the conditions described previously. Ten hours after transfection, cells were washed with PBS and incubated for 30 hours in serum-free medium (37 °C, 5% CO_2). Untreated fibroblasts were processed in the same conditions. Subsequently, cells were fixed in ice-cold methanol (5 minutes at –20 °C) and washed twice in PBS. Cells were permeabilized in PBS supplemented with 3% bovine serum albumin and 0.1% Triton for 1 hour at room temperature before being incubated overnight at 4 °C in permeabilization buffer containing (rabbit anti-γ-tubulin (1:1,000), mouse monoclonal anti-acetylated tubulin (1:1,000); Sigma-Aldrich) primary antibodies. After three washes with PBS, cells were incubated for 1 hour at room temperature in permeabilization buffer containing secondary antibodies (Alexa-Fluor 594– and Alexa-Fluor 488– conjugated goat anti-rabbit IgG (1:1,000) and goat anti-mouse IgG (1:1,000); Invitrogen, Life Technologies, St Aubin, France) followed by three washes with PBS. A mounting media containing 4′,6-diamidino-2-phenylindole (DAPI) (DAPI Fluoromount G; Southern Biotech, Birmingham, AL) was used to label nuclei. Immunofluorescence images were obtained using a Leica DM IRBE microscope and a MicroPublisher 3.3 RTV camera (Q-Imaging France, Bayonne, France). The final images were generated using the Cartograph version 7.2.3 (Microvision Instruments, Evry, France) and ImageJ (National Institutes of Health, Bethesda, MA). The percentage of ciliated cells was calculated from two independent experiments (n > 200 cells for each cell line). The significance of variations among samples was estimated using the protected list significant difference of Fisher according to the significance of the analysis of variance test (Statview Software, version 5).

Acknowledgments. We thank Sophie Massicot, Jerome Denard and Fedor Svinartchouk, Raphaelle Desvaux, and Nicolas Goudin for technical assistance. We are grateful to A.J. Mason and B. Bechinger for the kind gift of LAH4-L1. We thank the Association Retina France and the Fondation de France/Berthe Fouassier for financial support of X.G. The authors declared no conflict of interest.

Supplementary Material

Figure S1. Evaluation of exon-skipping efficiency using AONs designed from the CEP290 mutant mRNA sequence (see Figure 2).
Figure S2. Visualization of AON-mediated correction of aberrant splicing.
Figure S3. AON transfection efficiency.
Figure S4. AON treatment of patient P_1 fibroblasts in the presence of emetine.
Figure S5. Relative expression levels of wild-type and mutant in total extracts and cytoplasmic fractions of AON-treated fibroblasts.
Materials and Methods.

1. Kaplan, J (2008). Leber congenital amaurosis: from darkness to spotlight. *Ophthalmic Genet* **29**: 92–98.
2. Hanein, S, Perrault, I, Gerber, S, Tanguy, G, Barbet, F, Ducroq, D *et al.* (2004). Leber congenital amaurosis: comprehensive survey of the genetic heterogeneity, refinement of the clinical definition, and genotype-phenotype correlations as a strategy for molecular diagnosis. *Hum Mutat* **23**: 306–317.
3. den Hollander, AI, Roepman, R, Koenekoop, RK and Cremers, FP (2008). Leber congenital amaurosis: genes, proteins and disease mechanisms. *Prog Retin Eye Res* **27**: 391–419.
4. den Hollander, AI, Koenekoop, RK, Yzer, S, Lopez, I, Arends, ML, Voesenek, KE *et al.* (2006). Mutations in the CEP290 (NPHP6) gene are a frequent cause of Leber congenital amaurosis. *Am J Hum Genet* **79**: 556–561.
5. Perrault, I, Delphin, N, Hanein, S, Gerber, S, Dufier, JL, Roche, O *et al.* (2007). Spectrum of NPHP6/CEP290 mutations in Leber congenital amaurosis and delineation of the associated phenotype. *Hum Mutat* **28**: 416.
6. Craige, B, Tsao, CC, Diener, DR, Hou, Y, Lechtreck, KF, Rosenbaum, JL *et al.* (2010). CEP290 tethers flagellar transition zone microtubules to the membrane and regulates flagellar protein content. *J Cell Biol* **190**: 927–940.
7. Coppieters, F, Lefever, S, Leroy, BP and De Baere, E (2010). CEP290, a gene with many faces: mutation overview and presentation of CEP290base. *Hum Mutat* **31**: 1097–1108.
8. van Ommen, GJ, van Deutekom, J and Aartsma-Rus, A (2008). The therapeutic potential of antisense-mediated exon skipping. *Curr Opin Mol Ther* **10**: 140–149.
9. Aartsma-Rus, A (2010). Antisense-mediated modulation of splicing: therapeutic implications for Duchenne muscular dystrophy. *RNA Biol* **7**: 453–461.
10. Friedman, KJ, Kole, J, Cohn, JA, Knowles, MR, Silverman, LM and Kole, R (1999). Correction of aberrant splicing of the cystic fibrosis transmembrane conductance regulator (CFTR) gene by antisense oligonucleotides. *J Biol Chem* **274**: 36193–36199.
11. Lacerra, G, Sierakowska, H, Carestia, C, Fucharoen, S, Summerton, J, Weller, D *et al.* (2000). Restoration of hemoglobin A synthesis in erythroid cells from peripheral blood of thalassemic patients. *Proc Natl Acad Sci USA* **97**: 9591–9596.
12. Noensie, EN and Dietz, HC (2001). A strategy for disease gene identification through nonsense-mediated mRNA decay inhibition. *Nat Biotechnol* **19**: 434–439.
13. Aartsma-Rus, A, van Vliet, L, Hirschi, M, Janson, AA, Heemskerk, H, de Winter, CL *et al.* (2009). Guidelines for antisense oligonucleotide design and insight into splice-modulating mechanisms. *Mol Ther* **17**: 548–553.
14. Mason, AJ, Martinez, A, Glaubitz, C, Danos, O, Kichler, A and Bechinger, B (2006). The antibiotic and DNA-transfecting peptide LAH4 selectively associates with, and disorders, anionic lipids in mixed membranes. *FASEB J* **20**: 320–322.
15. Hammond, SM and Wood, MJ (2011). Genetic therapies for RNA mis-splicing diseases. *Trends Genet* **27**: 196–205.
16. Wang, GS and Cooper, TA (2007). Splicing in disease: disruption of the splicing code and the decoding machinery. *Nat Rev Genet* **8**: 749–761.
17. Skordis, LA, Dunckley, MG, Yue, B, Eperon, IC and Muntoni, F (2003). Bifunctional antisense oligonucleotides provide a trans-acting splicing enhancer that stimulates SMN2 gene expression in patient fibroblasts. *Proc Natl Acad Sci USA* **100**: 4114–4119.
18. Soret, J, Gabut, M and Tazi, J (2006). SR proteins as potential targets for therapy. *Prog Mol Subcell Biol* **44**: 65–87.
19. Sumanasekera, C, Watt, DS and Stamm, S (2008). Substances that can change alternative splice-site selection. *Biochem Soc Trans* **36**(Pt 3): 483–490.
20. Goemans, NM, Tulinius, M, van den Akker, JT, Burm, BE, Ekhart, PF, Heuvelmans, N *et al.* (2011). Systemic administration of PRO051 in Duchenne's muscular dystrophy. *N Engl J Med* **364**: 1513–1522.
21. Cirak, S, Arechavala-Gomeza, V, Guglieri, M, Feng, L, Torelli, S, Anthony, K *et al.* (2011). Exon skipping and dystrophin restoration in patients with Duchenne muscular dystrophy after systemic phosphorodiamidate morpholino oligomer treatment: an open-label, phase 2, dose-escalation study. *Lancet* **378**: 595–605.
22. Highleyman, L (1998). FDA approves fomivirsen, famciclovir, and Thalidomide. Food and Drug Administration. *BETA*: **5**.

23. Cideciyan, AV (2010). Leber congenital amaurosis due to RPE65 mutations and its treatment with gene therapy. *Prog Retin Eye Res* **29**: 398–427.
24. Chang, B, Khanna, H, Hawes, N, Jimeno, D, He, S, Lillo, C *et al.* (2006). In-frame deletion in a novel centrosomal/ciliary protein CEP290/NPHP6 perturbs its interaction with RPGR and results in early-onset retinal degeneration in the rd16 mouse. *Hum Mol Genet* **15**: 1847–1857.
25. Menotti-Raymond, M, David, VA, Schäffer, AA, Stephens, R, Wells, D, Kumar-Singh, R *et al.* (2007). Mutation in CEP290 discovered for cat model of human retinal degeneration. *J Hered* **98**: 211–220.
26. Tinsley, JM, Fairclough, RJ, Storer, R, Wilkes, FJ, Potter, AC, Squire, SE *et al.* (2011). Daily treatment with SMTC1100, a novel small molecule utrophin upregulator, dramatically reduces the dystrophic symptoms in the mdx mouse. *PLoS ONE* **6**: e19189.
27. Moorwood, C, Lozynska, O, Suri, N, Napper, AD, Diamond, SL and Khurana, TS (2011). Drug discovery for Duchenne muscular dystrophy via utrophin promoter activation screening. *PLoS ONE* **6**: e26169.
28. Tian, Q, Stepaniants, SB, Mao, M, Weng, L, Feetham, MC, Doyle, MJ *et al.* (2004). Integrated genomic and proteomic analyses of gene expression in Mammalian cells. *Mol Cell Proteomics* **3**: 960–969.
29. Wang, D (2008). Discrepancy between mRNA and protein abundance: insight from information retrieval process in computers. *Comput Biol Chem* **32**: 462–468.
30. Papon, JF, Perrault, I, Coste, A, Louis, B, Gérard, X, Hanein, S *et al.* (2010). Abnormal respiratory cilia in non-syndromic Leber congenital amaurosis with CEP290 mutations. *J Med Genet* **47**: 829–834.
31. Vandesompele, J, De Preter, K, Pattyn, F, Poppe, B, Van Roy, N, De Paepe, A *et al.* (2002). Accurate normalization of real-time quantitative RT-PCR data by geometric averaging of multiple internal control genes. *Genome Biol* **3**: RESEARCH0034.

Supplementary Information accompanies this paper on the Molecular Therapy–Nucleic Acids website (http://www.nature.com/mtna)